AD-A090 412 ABERDEEN PROVING GROUND MD MATERIEL TESTING DIRECTORATE F/G 14/2
ELECTRON MICROSCOPY USED FOR FRACTURE MODE IDENTIFICATION,(U)
JUN 80 C R KLARICH, R L HUDDLESTON, M J DRABO

UNCLASSIFIED NL

END
DATE FILMED
11-80
DTIC

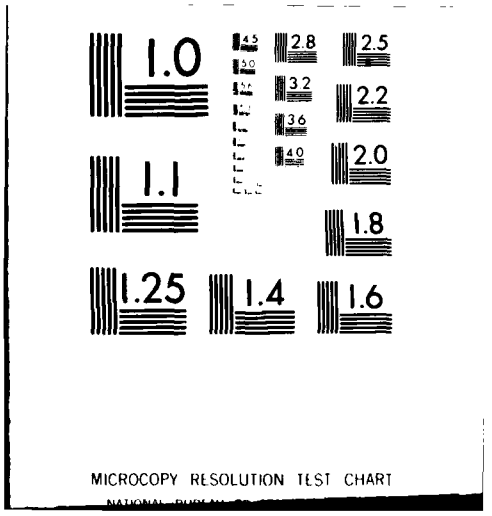
1.0
1.1
1.25
1.4
1.6
1.8
2.0
2.2
2.5
2.8
3.2
3.6
4.0
4.5
5.0
MICROCOPY RESOLUTION TEST CHART

ELECTRON MICROSCOPY USED FOR FRACTURE MODE IDENTIFICATION (U)

CHARLES R. KLARICH, R. L. HUDDLESTON AND M. J. DRABO
Materiel Testing Directorate
Aberdeen Proving Ground, Maryland 21005

INTRODUCTION

Metallurgical failure analysis represents a technology which combines the knowledge of many scientific and engineering disciplines. During these times of increasing product liability litigation, interest in failure analysis has intensified. The failure analyst is asked to identify the cause of catastrophic failures in many different materials. During past years at the proving ground, the list of materiel evaluated includes such diverse items as a cargo truck firewall and 175 mm gun tubes. The disciplines required include, metallography, chemical analysis, light and electron microscopy, stress analysis, and the measurement of mechanical properties.

Effective failure analysis depends on a combination of factors; these include the assessment of prior manufacturing and service history, a knowledge of materials and available test methodology and finally, how these factors interrelate with the applied loads and design intent (1). Conventional failure analysis begins with a visual examination of the item to evaluate the material response to fracture. The analyst uses all the disciplines outlined above to focus the investigation on the cause of failure. A powerful tool in the analysis is the Scanning Electron Microscope (SEM) and the discipline called fractography.

Fractography then, may be described as the study of a fracture surface to determine the micromechanisms of fracture. This information can help to determine the cause of the failure. Visual examination of metal fractures goes back to the sixteenth century.

An optical microscope was first used in the examination of metallic fractures by Reaumer in 1722 (2), but the first detailed use of optical fractography was done years later by Zappfe and Clogg in 1945 (3). They studied numerous fractures made in steels and characterized their appearance. The introduction of commercial Transmission Electron Microscopes (TEM) in the 1960's accelerated and development of fractography. The actual fracture surface cannot be viewed with a TEM because the electron beam must pass through the sample, but replication techniques were devised. Sample preparation was difficult and artifacts on the fracture surface were a problem. The SEM is an instrument that essentially bridges the gap between the optical microscope and the TEM. Today fracture surfacescan be viewed directly after the proper cleaning techniques are used by the microscopist. A second advantage is the depth of focus obtained with the SEM compared to optical techniques. A rough fracture surface will remain in focus at magnifications of 5000X.

This paper describes the analysis of two barrel support jacket failures from the M2 machine gun analyzed at the Materiel Testing Directorate, Aberdeen Proving Ground (APG), utilizing the SEM. Electron microscopy is a diagnostic tool primarily used to view fracture topography and identify fracture mode. The fracture modes are classified primarily as ductile or brittle plus fatigue, and intergranular variations. The following examples illustrate ductile, brittle, intergranular and fatigue failure mechanisms.

Ductile failure is characterized by the formation of voids on the fracture surface that plastically coalesce to form dimples. This micromechanism is termed microvoid coalescence. The fractograph of a tensile sample machined from a plain carbon AISI 1018 steel shows this type of failure. The size of the dimples is determined by number and location of the microvoids that are nucleated. The nucleation sites are inclusions, second phase particles, or grain boundaries.

Figure 1. A Fractograph of a 1018 Plain Carbon Steel Tensile Bar Which Shows Ductile-Dimpled Rupture. Magn: 2400X

394

An example of a brittle failure is the fracture surface observed on a sintered tungsten material (4). The slug was fabricated from a tungsten powder that was liquid sintered with a nickel-iron binder. The material was then swagged 25%. A slug of this material was fractured with a stress wave and then viewed with the SEM.

Figures 2 and 3. A Fractograph of the Liquid Sintered Tungsten Material Which Shows Cleaved Tungsten Particles and Round or Oblong Flat Facets in a Ductile-Iron Matrix. Magn: 1400X and 3500X

Electron fractography showed the fracture mode was brittle. Three different micromechanisms were observed in the material. The tungsten particles failed by cleavage and intergranular fracture. Cleavage steps were observed on numerous cleavage planes. The flat oblong or round areas were regions of intergranular rupture. These facets can result from air being trapped in the liquid sintered material. The third type of micromechanism was the ductile failure of the nickel-iron matrix.

A brittle fracture with an intergranular mechanism was noted on a spider universal joint from the Infantry Fighting Vehicle (IFV). The U-joint was case carburized and was in service for a total of 474 miles when failure occurred (Fig 4).

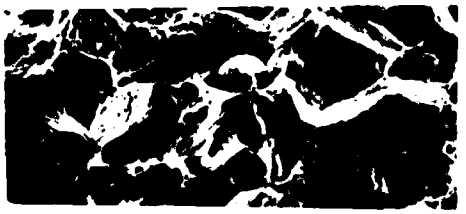

Figure 4. Intergranular Fracture, U-Joint. Magn: 700X

Figure 5. Fatigue Striations Observed on Axle Shaft. Magn: 350X

Visual and low power optical examination did not reveal the intergranular fracture mechanism. The extent of the brittle cracking was a function of the case depth.

The next type of fracture to be illustrated is the fatigue failure. These failures are characterized by a striated fracture surface. The number of cyclic load applications are approximated from the striation spacing at different locations on the fracture surface. A recent example of a fatigue failure occurred during the initial production test (IPT) of a rough terrain forklift (5). Several rear axle shafts failed catastrophically during reliability testing. The axle shafts broke in the splined end from reverse torsional fatigue (see Figure 5).

The variety of material failures encountered at the proving ground range from alloy steels to sintered tungsten. Electron fractography is used to determine the micromechanisms on the fracture surface. This information is correlated with mechanical property information and the microstructure of the failed item to determine the cause of failure. Corrective action is then recommended. A typical example of the failure technique used at APG is shown in the analysis of the barrel support jacket failures. The analysis uses an integrated approach that evaluates background data, service history, and visual examination before employing other analytical methods to focus on the cause of the failure. The scanning electron microscope is the central core of the analysis.

BACKGROUND - BARREL SUPPORT JACKET FAILURES

A Blank Firing Attachment (BFA) M19 was developed for the M2 Heavy Barrel Machine Gun (HBMG) Cal .50 weapon.

Figure 6. View of M2 Machine Gun with Blank Firing Attachment.

The BFA is used in tactical field training exercises as a Weapon Effects Signature Simulator (WESS) to support the real train engagement simulation system (6-8). The blank firing attachment provides an effects signature from the position of the firing weapon. The blank firing attachment caps the barrel and generates a recoil with the blanks. This activates the bolt mechanism to eject the spent blank and feeds an additional blank into the chamber. The M2

is designed to fire 450 rounds/minute with conventional ammunition. It operates at 700 rounds/minute with the blanks. More force is generated firing the blank ammunition and the barrel also has more vertical whip. The barrel support jackets each had 5-6000 rounds fired with the blank firing attachment in place. The total number of rounds on the barrel supports was not determinable. The machine guns are periodically rebuilt so the failed components were probably on several different weapons since manufacture. Two barrel support jackets failed during testing of blank firing attachment. The cracked barrel supports caused misalignment of the front barrel bushing in the M2 .50 cal HBMG. This misalignment caused the barrel to bind in the bushing thereby causing weapon stoppages.

TEST TECHNIQUES

A. Electron Microscopy.

The barrel support jackets were visually examined and sectioned before sputter etching. The fracture surfaces were coated with black residue which was the result of a gas wash from the firing of the M2 machine gun. Repeated sputter etchings were required. The sputtering device provides etching-cleaning of samples by immersing the work in a charged plasma field. Organic material is removed as is some of the base material itself.

The fractographic examination of all samples was conducted with an Advanced Metals Research (AMR) Model 1200 Scanning Electron Microscope (SEM) with an accelerating voltage of 25 KV. Resolution of the instrument is 100 angstroms. Qualitative chemical analysis and X-ray mapping was done with an energy dispersive X-ray spectrometer attached to the SEM.

B. Microscopy.

A microstructural analysis was conducted on samples of each broken barrel support jacket with a metallograph. A sample used for microscopic examination was also examined with the SEM to chemically identify a substance on the fracture surface.

C. Hardness Measurements.

Brinell hardness, 500 Kgm load, was determined on each barrel support jacket near the failure.

D. Quantitative Chemical Analysis.

An X-ray spectrometer was used to determine the chemical analysis of the barrel support jackets. The carbon level was determined with a gasometric carbon analyzer.

RESULTS

A. Visual Examination/Electron Microscopy.

BSJ labeled Number 1 had a through crack in a web section near the center of the part.

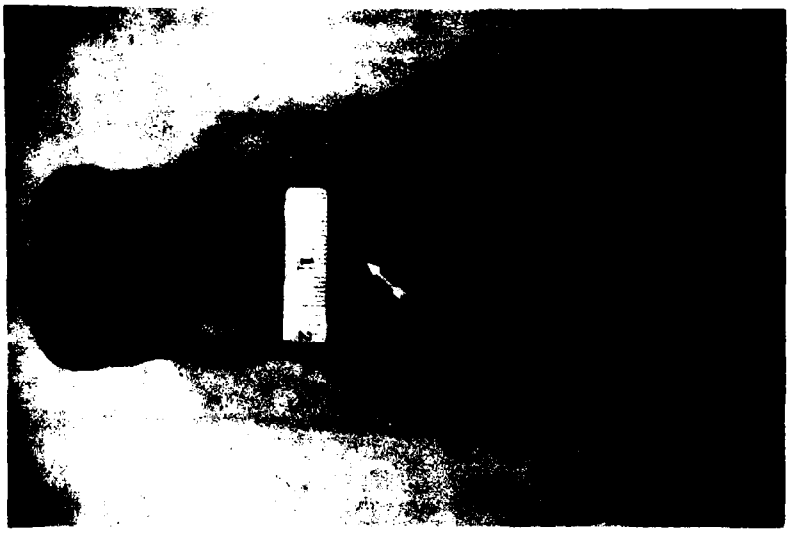

Figure 7. A View of BSJ Number 1 Which Shows the Location of the Through Crack.

The second BSJ had three sequential cracks in the webs at the forward end of the part. Each of these cracks was a through crack.

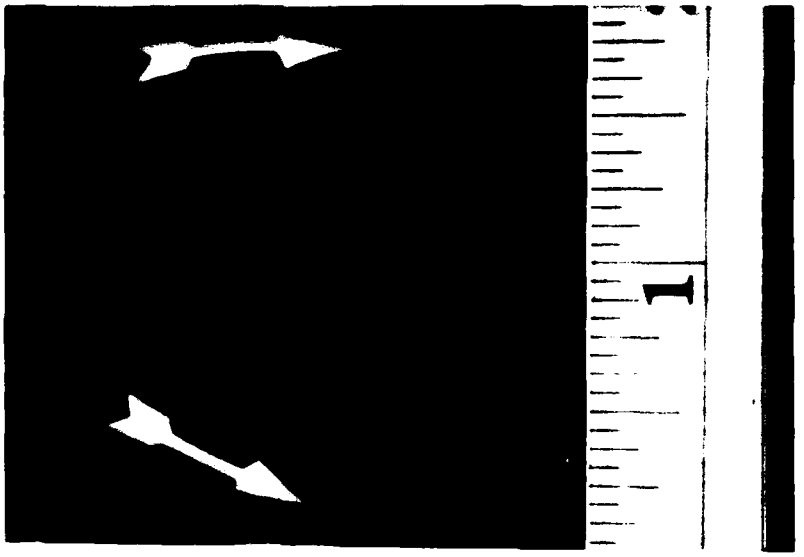

Figure 8. A Photograph Which Shows Two of the Cracked Webs in BSJ Number 2.

Visual examination of the fracture surfaces did not lead to a positive identification of the fracture mode. SEM analysis of the fracture surfaces was hampered by a black residue which resulted from the gas wash of the M2 machine gun. The fracture surface on BSJ Number 1 contained three distinct zones. The origin of failure on BSJ Number 1 was a flat zone on the fracture surface. Evidence of fatigue striations was obliterated by burnishing of the mating fracture surface. The remainder of the fracture surface visually appeared as an intergranular fracture. The periphery of the fracture surface on the side away from the flat zone contained a minute shear lip. Electron fractography showed the mating fracture surfaces had rubbed together and obliterated the fracture topography.

(399)

Figure 9. A Fractograph of BSJ Number 1 Which Shows the Fracture Surface Damage. The Fracture was not Intergranular. Magn: 800X

The fracture surfaces from BSJ Number 2 showed a ductile-dimpled fracture surface formed by microvoid coalescence. Manganese sulfide inclusions were visible in several of the dimples. This fracture topography is indicative of a tensile failure.

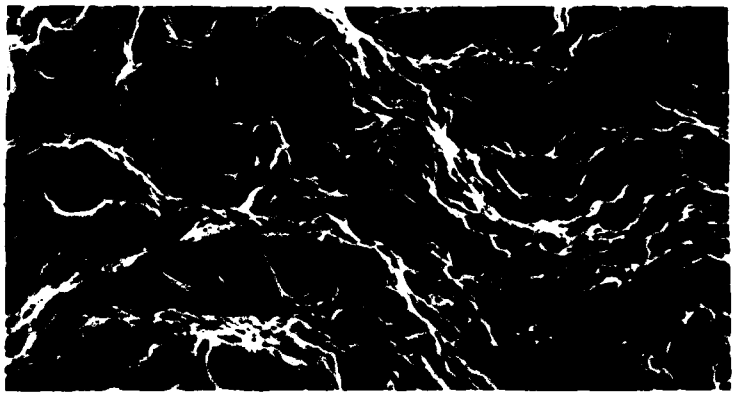

Figure 10. The Fracture Surface of BSJ Number 2 Showed a Ductile-Dimpled Fracture Surface Formed by Microvoid Coalescence. Magn: 1320X

B. Microstructural Analysis.

The microstructure of BSJ Number 1 at the fracture surface showed a non-metallic inclusion at the fracture surface and manganese sulfide inclusions throughout the matrix. The etched matrix material showed the BSJ Number 1 was made from a pearlitic malleable iron. The pearlitic matrix was partially spheroidized by a tempering treatment in the manufacturing sequence. The irregular nodules of temper carbon graphite are typical of a malleable iron. The graphite conforms to ASTM Type III temper carbon.

Figure 11. A Micrograph of BSJ Number 1 Which Shows a Pearlitic Malleable Iron Matrix. Note the Non-Metallic Inclusion on the Fracture Surface. Magn: 200X Etchant: 2% Nital

Note the area of ferrite adjacent to the inclusion on the fracture surface. This indicates the defect was present during the annealing of the material. The inclusion or the ferritic layer extended 87% across the length of the fracture surface. This caused a zone of weakness across the web that failed in BSJ Number 1. This area was the flat region viewed on the fracture surface. The white constituent around the temper carbon nodules is ferrite. The formation of a complete bull's-eye structure was minimized by a short annealing time, so the envelopes of free ferrite around the graphite nodules are not completely formed.

401

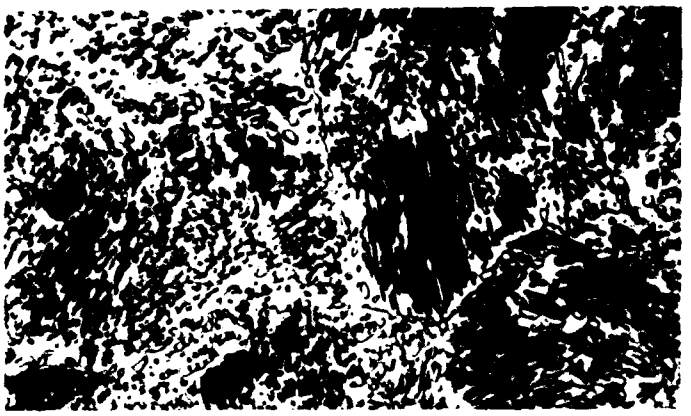

Figure 12. A Micrograph of the Matrix Material of BSJ Number 1 Shows a Pearlitic Structure that was Partially Speriodized by a Tempering Treatment. The Gray Particles are MNS Inclusions. Magn: 1400X Etchant: 2% Nital

Microstructural examination of BSJ Number 2 also showed it was pearlitic malleable iron. The pearlitic matrix was partially spheroidized by the tempering treatment. No large non-metallic inclusions were seen on the fracture surface of BSJ Number 2.

Figure 13. A Micrograph of the Fracture Surface on BSJ Number 2 Which Shows the Irregular Fracture Path Typical of a Ductile-Dimple Rupture. Magn: 200X Etchant: 2% Nital

The fracture path followed the low strength ferrite grains and temper carbon nodules across the cross-section of the web in BSJ Number 2.

C. Chemical Analysis.

The X-ray spectrochemical analysis of the barrel support jackets showed they were both a malleable iron material. The carbon and manganese content were typical for a pearlitic malleable iron. The silicon content was slightly higher than normal.

Table 1. Chemical Analysis of Barrel Support Jackets No. 1 and 2

BSJ Part No.	% Element, Wt C	MN	P	S	Si	Ni	Cr	Mo	V	Cu
1	2.46	0.41	0.07	0.14	1.78	0.14	0.04	0.01	0.03	0.08
2	2.45	0.43	0.07	0.15	1.82	0.14	0.04	0.01	0.03	0.08
Typical Pearlitic Malleable	2.00-2.70	0.25-1.25	0.05 max	0.03-0.18	1.00-1.75	-	-	-	-	-

D. Elemental Mapping.

A sample that was used for microstructural analysis was also for elemental mapping. The area of interest was the inclusion seen on the fracture surface on BSJ Number 1.

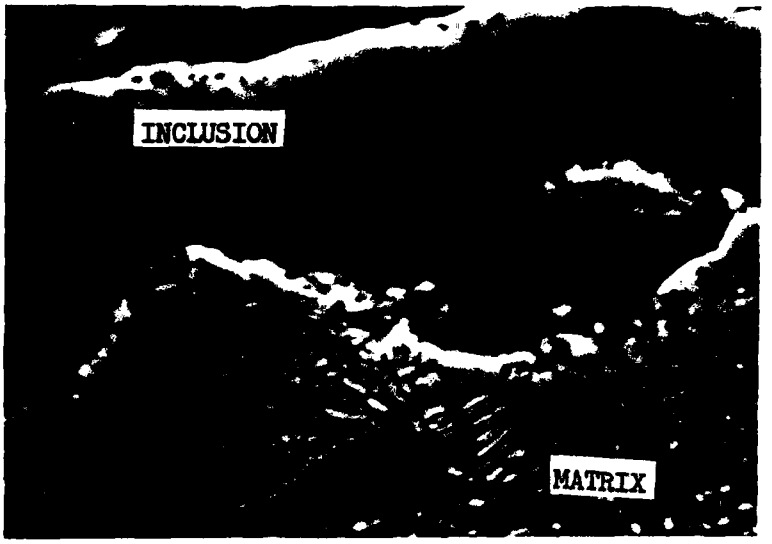

Figure 14. A SEM View of the Inclusion at the Fracture Surface on BSJ Number 1. Magn: 1800X

The platelets seen in the matrix are pearlite lamellae. These are alternate layers of ferrite and iron carbide. The globular particles in the matrix are manganese sulfide inclusions. Acquiring an X-ray energy dispersive spectrum from the fracture surface inclusion showed the elements Fe, Mn and Si were present. Elements on the periodic chart below atomic Number 13 (aluminum) are not detected. Elemental mapping was conducted for the elements Fe, Mn, and Si.

The iron concentration was distributed uniformly throughout the malleable iron and the inclusion. The iron concentration was the highest of the three elements mapped. Manganese was noted over the entire area that was mapped with the highest concentrations at the inclusions in the malleable iron. The silicon was concentrated near the fracture surface in the region examined.

E. Hardness.

The Brinell hardness (500 Kgm load) was taken on various sections of BSJ's 1 and 2 near the through cracks. The hardness of BSJ Number 2 was lower than the typical pearlitic malleable iron.

(4M)

Table 2. Brinell hardness (500 Kgm Load) of BSJ's Labeled 1 and 2

BSJ Part No.	Section I. D.	BHN (500 Kgm Load)
1	A	158, 158, 150
1	B	158, 158, 158
2	A	130, 130, 140
2	B	124, 143, 136
2	C	143, 136
2	D	130, 143, 136
2	F	136, 150, 136
2	E	136, 143, 150

Note: The typical hardness range for a pearlitic malleable-iron grade 40010 ranges from BHN 149-197. Other grades of pearlitic malleable iron have higher hardness ranges.

DISCUSSION

The fatigue process normally proceeds in two stages - initiation of the crack and crack propagation. Barrel support jacket Number 1 failed by fatigue in a web section thicker than the failed webs in BSJ Number 2. A casting defect weakened the cross-section and allowed a fatigue crack to initiate in the web. The layer of ferrite adjacent to the defect indicates that it was present during the annealing process. The inclusion was identified by the elemental mapping technique as an iron compound with Mn and Si in solid solution. The initiation of cracking at the inclusion most probably occurred during the initial use of the BSJ before the addition of the blank firing attachment. The rate of fatigue crack growth is controlled primarily by the intensity of loading which is described by the stress intensity factor (K). The crack growth rate was low during the initial use of the BSJ on the M2 HBMG, but addition of the blank firing attachment increased the stress intensity factor at the defect and allowed the crack to propagate to failure in less than 6000 cycles.

The stresses on the BSJ are increased when the M2 machine gun is operated with the blank firing attachment. The gun is operated at 700 rounds/minute compared to the design rate of 450 rounds/minute and has the extra weight of the attachment. The increased stress in combination with the thin web cross-section and lower than average hardness resulted in a tensile failure of BSJ Number 2. SEM

405

examination confirmed the tensile micromechanism of failure. The BSJ was also bent by the forces generated during testing the blank firing attachment.

The entire material failure analysis process is an integration of the bits of information gained from electron microscopy, microstructural analysis, service conditions, hardness testing, visual examination, and X-ray elemental mapping. Analysis of field failures is not as straight forward as the analysis of laboratory produced fractures. The discovery of a casting defect at the fracture surface of BSJ Number 1 by microstructural structure analysis pinpointed the origin of failure. This information plus the knowledge of the service conditions in combination with the other data lead to the determination the BSJ Number 1 failed in fatigue. The electron microscopy data was conclusive in the analysis of BSJ Number 2. These three webs failed in a tensile mode and no burnishing of the fracture surface was in evidence. The other information, expecially the hardness data, corroborates the SEM analysis. Electron microscopy is essential in the analysis of materiel field failures to reduce the uncertainty and also make positive identifications of the fracture mode.

CONCLUSIONS

Barrel support jacket Number 1 failed in fatigue caused by an increased loading due to the blank firing attachment and a casting defect that weakened the web.

Barrel support jacket Number 2 failed in a ductile rupture mode caused by a combination of a higher than normal loading, a thin cross-sectional area and lower than normal hardness for a pearlitic malleable iron part. The micromechanism of the failure was microvoid coalescence.

CORRECTIVE ACTION RECOMMENDED

An improved casting technique be used in the manufacture of the barrel support jackets.

Only thick webbed barrel support jackets be used on the M2 machine gun when the blank firing attachment is used.

The depot rebuild program for the M2 machine gun use only the thick web barrel support jackets.

Cracks not be allowed in the barrel support jackets used in the depot rebuild operation.

40a

SUMMARY

Electron microscopy is essential in the analysis of materiel service failures to reduce the uncertainty and also to make positive identifications of the fracture modes. The examples given illustrate the way the SEM is used to characterize fracture topographies. The SEM is at the core of the analytical procedure which focuses diverse bits of information into determining the cause of failure. The analysis includes prior service history, manufacturing methods, mechanical properties, metallurgy, and the SEM. Each failure requires a specific combination of tests to solve the problem. The tests are complimentary and result in an intense examination of the critical areas of interest. The payoff is correct identification of the cause of failure and corrective action which results in improved Army materiel.

REFERENCES

(1) Drabo, M. J., "Analytical Processes for Failure Analysis", Minutes 1979 TECOM Instrumentation Conference, p. 271.

(2) Reaumer, "L'Art De Converter Le Fer En Acier", Paris 1722.

(3) Zappfe, C. A., and Clogg, M., "Fractography - A New Tool for Metallurgical Research", Trans ASM Vol 34 (1945) p. 71.

(4) Klarich, C. R., "Ballistic Technology - Fragmenting Warheads", Physical Test Branch Report 76-M-75, MTD, APG, Maryland.

(5) Faller, J. G., "IPT of 4000 Pound Rough Terrain Forklift", Physical Test Branch Report 79-M-55, MTD, APG, Maryland.

(6) Letter Requirement for Blank Firing Adaptor for Cal .50 Machine Gun M2 Between Commander, U.S. Army Training and Doctrine Command and Commander, U.S. Army Materiel Development and Readiness Command, 1976.

(7) Maule, M., "Development Test II (PQT-G) of Blank Firing Adaptor for M2 Machine Gun and Product Improvement Test of Cal .50 Blank Ammunition", Test Report APG-MT-5346, Aberdeen Proving Ground, Maryland.

(8) Klarich, C. R., "Metallurgical Analysis of Two Failed Barrel Support Jackets", Physical Test Branch Report 79-M-47, MTD, APG, Maryland.